Berry-phase-like effect of thermo-phonon transport in optomechanics

Wenjie Nie [1,*] Guoyao Li,[1] Xiyun Li,[1] Aixi Chen,[2,†] Yueheng Lan,[3,‡] and Shi-Yao Zhu[4]

[1]*Department of Applied Physics, East China Jiaotong University, Nanchang 330013, China*
[2]*Department of Physics, Zhejiang Sci-Tech University, Hangzhou 310018, China*
[3]*Department of Physics, Beijing University of Posts and Telecommunications, Beijing 100876, China*
[4]*Department of Physics, Zhejiang University, Hangzhou 310027, China*

We investigate thermo-phonon transport and its nontrivial Berry-phase-like effect in an optomechanical system with a squeezed vacuum injection. By taking the cumulant generation function approach the exact expressions of the thermo-phonon flux and optomechanical Berry phase are derived analytically. Further, the quantum master equation approach is invoked to verify the analytical results of the transport properties. It is shown that the steady-state thermo-phonon flux can be modulated by varying optically the nonequilibrium characteristics of the system via the squeezed vacuum. In particular, an adiabatic modulation of squeezing parameters induces an optomechanical Berry-phase-like effect and as a result provides an additional geometric phonon response across the macroscopic mechanical motion near the quantum regime, which can also be seen as a consequence of the asymmetric jumping probability between transition associated with phonon absorption and emission in a thermal bath. The present method and results are general and can be straightforwardly extended to any multimode oscillator systems and therefore pave the way to the thermal noise energy harvesting and rectification in coupled oscillator systems with inertial terms.

I. INTRODUCTION

Recently, cavity optomechanical systems have emerged as an unique platform for exploring theoretically and experimentally the quantum effect in macroscopic motions, i.e., the ground-state cooling [1–5], mechanical coherence and continuous-variable (CV) entanglement [6–15], phonon lasing or mechanical squeezing [16,17], nonclassical state preparation [18,19], nonlinear quantum optomechanical effects [20–25], and so on. These fascinating quantum phenomena in macroscopic systems originate from significant interactions between light and mechanical oscillators via radiation pressure, which effectively counters the dissipation imposed by the environment [26]. Potential application of cavity optomechanics includes weak-force sensing and measurements [27–29], quantum wavelength conversion [30,31], quantum illumination [32], nonreciprocal energy transfer [33], and optomechanical transistor [34].

In addition, the intriguing thermodynamic aspect of cavity optomechanical systems has attracted extensive attention in the study of optomechanical quantum heat engines [35–41] and pump cooling [42], nonreciprocal optomechanical heat transport [43–45] and irreversible entropy production of quantum systems [46,47]. Despite these efforts, quantization of heat and phonon transfers in nonequilibrium optomechanical systems coupled to zero-temperature or nonthermal environments remains unexplored, the clarification of which helps one identify general features of transports in nonequilibrium context [48–53] and design micro-nanoscale thermal rectifiers and logic gates [54–61]. In particular, when a cyclic two-parameter modulation of the driven optomechanical system is established, how to calculate nontrivial Berry phase of the quantum system is a very interesting problem, which would enable flexible dynamical control of nonequilibrium heat noise flow [62–67] and therefore has much application in phononics and optomechanics [26,52].

For this purpose, in this paper, we aim to study the universal Berry-phase in a CV optomechanical system, which can induce an additional geometric thermo-phonon pumping. We describe the system dynamics by converting the quantum Langevin equation into a *c*-number Langevin equation including commutator relations of the fluctuation operators [68,69]. And then we solve the Fokker-Planck (FP) equation [70–72] corresponding to the *c*-number Langevin equation and derive the general expressions of the steady-state thermo-phonon flux and the optomechanical Berry curvature by using the cumulant generating function (CGF) approach. We confirm further the existence of geometric thermo-phonon pumping by modulating slowly the phase of the squeezed vacuum and find that an additional geometric phonon response can be realized when the system works near the quantum region. The CGF approach is numerically tested for the exact results of the quantum master equation (QME) and is giving correct predictions for the geometric phonon transport in the weakly coupling regime. The results attained here pave the way to the thermal noise energy harvesting and rectification in a quantum optomechanical system by means of all-optical regulation.

*niewenjiezhu@sina.cn
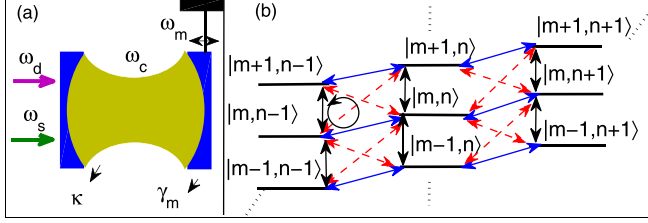†aixichen@zstu.edu.cn
‡lanyh@bupt.edu.cn

FIG. 1. (a) Schematic illustration of an optomechanical system with squeezed vacuum injection. (b) Level diagram of the linearized Hamiltonian (1). $|m, n\rangle$ denotes the state of m photons and n phonons in the displaced frame. The blue (black) lines with double arrows denote the transitions between the states due to the coupling with the thermal (vacuum) bath. Black ring with an arrow denotes an optimal route of energy transfers from the mechanical mode to the optical mode via the optomechanical coupling channels (red dashed lines with double arrows). In the nonequilibrium steady state, the quantum state, i.e., $|m, n\rangle$, does not change any more and a steady-state thermo-phonon flux J_p flows from the thermal bath into the system.

II. THE MODEL

We consider a standard optomechanical system sketched in Fig. 1(a), where a movable mechanical oscillator is coupled to a cavity field with frequency ω_c and decay rate κ. The optical cavity is driven by a strong input laser with frequency ω_d and injected by a squeezed vacuum field with central frequency $\omega_s = \omega_c$. The total Hamiltonian of the system in the frame rotating at the driving frequency ω_d reads (setting $\hbar = 1$) [26], $H_t = (\omega_c - \omega_d)\hat{a}^\dagger\hat{a} + \omega_m\hat{b}^\dagger\hat{b} - G_0\hat{a}^\dagger\hat{a}(\hat{b}^\dagger + \hat{b}) + i\Omega(\hat{a}^\dagger - \hat{a})$, where $\hat{a}$ and $\hat{b}$ are the annihilation operators belonging to the cavity field and the oscillator (with mass m, frequency ω_m and decay rate γ_m), respectively; and satisfy the commutator relation $[\hat{a}, \hat{a}^\dagger] = 1$ and $[\hat{b}, \hat{b}^\dagger] = 1$, respectively. Ω is the driving amplitude of the cavity mode with $|\Omega| = \sqrt{\frac{2P_d\kappa}{\hbar\omega_d}}$; $G_0 = (\omega_c/L_0)\sqrt{\hbar/(2m\omega_m)}$ is the single-photon optomechanical coupling strength. P_d is the power of laser and L_0 is the cavity length.

For strong driving, we can decompose each operator into a sum of the steady-state value and a small fluctuating part, i.e., $\hat{O} = O_s + \delta\hat{O}$ ($O = a, b$). Then, the linearized Hamiltonian is given by

$$H_L = \Delta\delta\hat{a}^\dagger\delta\hat{a} + \omega_m\delta\hat{b}^\dagger\delta\hat{b} - G_1(\delta\hat{a}^\dagger + \delta\hat{a})(\delta\hat{b}^\dagger + \delta\hat{b}), \quad (1)$$

where $\Delta = \omega_c - \omega_d - G_0(b_s + b_s^*)$ and $G_1 = G_0 a_s$ are the effective cavity detuning and optomechanical coupling, respectively; $a_s = \Omega/(\kappa + i\Delta)$ and $b_s = iG_0|a_s|^2/(\gamma_m + i\omega_m)$. In the present system, we always focus on the weak optomechanical coupling regime, which ensures that the nonlinear effects in the system is marginal. In this case, the quantum fluctuation dynamics of the system can be described by the Heisenberg-Langevin equations of motion

$$\delta\dot{\hat{b}} = (-i\omega_m - \gamma_m)\delta\hat{b} + iG_1(\delta\hat{a}^\dagger + \delta\hat{a}) + \sqrt{2\gamma_m}\hat{b}_{in}(t),$$

$$\delta\dot{\hat{a}} = (-i\Delta - \kappa)\delta\hat{a} + iG_1(\delta\hat{b}^\dagger + \delta\hat{b}) + \sqrt{2\kappa}\hat{a}_{in}(t). \quad (2)$$

The correlation of the thermal noise is $\langle\hat{b}_{in}(t)\hat{b}_{in}^\dagger(t')\rangle = (n_t + 1)\delta(t - t')$, where $n_t = \exp(\frac{\hbar\omega_m}{k_B T} - 1)^{-1}$ with k_B being the Boltzmann constant and T the temperature. The nonzero

Markovian correlations of the squeezed vacuum [73–75] are $\langle\hat{a}_{in}(t)\hat{a}_{in}(t')\rangle = M_s\delta(t - t')$, and $\langle\hat{a}_{in}(t)\hat{a}_{in}^\dagger(t')\rangle = (N_s + 1)\delta(t - t')$, where $M_s = (1/2)\sinh(2r)e^{i\theta}$ and $N_s = \sinh^2(r)$ in the case of pure squeezing and r and θ are the strength and the phase of the squeezing, respectively.

The quantities of interest to us here are the total amount of heat Q_h and the corresponding thermal phonon flux, flowing from the thermal bath into the optomechanical system in a given time duration τ, in a nonequilibrium steady state with m photons and n phonons in the displaced frame, shown in Fig. 1(b). From a quantum dynamics point of view, when the system works in the steady state near the quantum regime, its quantum state, i.e., $|m, n\rangle$, still has certain probability of transiting to its adjacent states and then jumps back to $|m, n\rangle$ by the coupling with thermal or vacuum baths as well as optomechanical interactions, i.e., $|m, n\rangle \rightarrow |m + 1, n - 1\rangle \rightarrow |m, n - 1\rangle \rightarrow |m, n\rangle$ marked by the black ring in Fig. 1(b). Physically, it is these transitions between quantum states of the optomechanical sub-system that mediate the energy transfer between the two sources on the energy scale of mechanical quantum. Further, our main concern is that the control parameters of the system are cyclically regulated, so that the transition probabilities between the quantum states are controlled dynamically and the geometric contribution of the thermo-phonon transport may be generated by a nontrivial Berry phase [62,65,76], similar to that in quantum mechanics [77,78]. It is noted that the study of Berry phase and Hannay angle in optomechanical system without the noises has been discussed in detail [79].

Here in order to reveal the main characteristics of noise flow in the open oscillator system, we focus on the heat transfer (Q_h) induced by the noise acting on the momentum of the mechanical oscillator, which can be defined as [65,80]

$$Q_h(\tau) = \hbar\omega_m \int_0^\tau [\hat{\xi}_p(t) - \gamma_m\hat{p}(t)]\hat{p}(t)dt, \quad (3)$$

where $\hat{\xi}_p(t) = i(\hat{b}_{in}^\dagger - \hat{b}_{in})/\sqrt{2}$ is the thermal noise related to the momentum of the oscillator $\hat{p} = i(\hat{b}^\dagger - \hat{b})/\sqrt{2}$. The heat Q_h can be identified as $Q_h = \hbar\omega_m N_{p0}$, with $N_{p0}(\tau) = \int_0^\tau [\hat{\xi}_p(t) - \gamma_m\hat{p}(t)]\hat{p}(t)dt$ being the number of the thermo-phonon. It is a fluctuating quantity and can be written as $N_{p0}(\tau) = -\gamma_m p_s^2\tau + \int_0^\tau [\hat{\xi}_p(t) - \gamma_m\delta\hat{p}(t)]\delta\hat{p}(t)dt$ in terms of the steady state value $p_s = (b_s - b_s^*)/(\sqrt{2}i)$ and the corresponding fluctuation $\delta\hat{p} = (\delta\hat{b} - \delta\hat{b}^\dagger)/(\sqrt{2}i)$. Obviously, the second term of N_{p0} is a little complicated but its average is always determined by the first and second moments of Eq. (2). Then, we can study the steady-state average thermo-phonon flux, i.e., $J_p = \lim_{\tau \to \infty}\langle N_{p0}(\tau)\rangle/\tau$, and its Berry-phase-like effect by solving the quantum operator equation (2). It is noted that the second moments of Eq. (2) should include the incommutability of the operators, which embodies the characteristics of the system in the quantum regime. Therefore, before solving the operator equation (2), we first convert it to a c-number Langevin equation, whose first and second moments should be identical with Eq. (2). This demands a unique relationship between the operators and the c-number Langevin equations, which can be attained by defining a correspondence between products of c-numbers and operators [68]. Considering the incommutability between operators in

Eq. (2), we choose the antinormal ordering $\delta\hat{b}$, $\delta\hat{a}$, $\delta\hat{b}^\dagger$, $\delta\hat{a}^\dagger$ and then derive two c-number Langevin equations for the c-number variables A and B such that the equations for their first and second moments are identical. In terms of the chosen ordering and according to Eq. (2), we have

$$\dot{B} = (-i\omega_m - \gamma_m)B + iG_1(A^* + A) + F_B(t),$$
$$\dot{A} = (-i\Delta - \kappa)A + iG_1(B^* + B) + F_A(t). \tag{4}$$

The functions F_A and F_B in Eq. (4) are again the typical Langevin noise with the expectation values

$$\langle F_k(t) \rangle = 0,$$
$$\langle F_k(t)F_l(t') \rangle = \langle 2D_{kl} \rangle \delta(t - t'), \tag{5}$$

where F_k and F_l can be either F_A or F_B. The diffusion coefficients D_{kl} should be determined by the requirement that the evolution equation for the second moments is identical to the corresponding operator equation. Using Eqs. (2), (4), and the commutator relation of the fluctuation operators, the nonzero c-number diffusion coefficients D_{kl} can be calculated with chosen ordering $\delta\hat{b}$, $\delta\hat{a}$, $\delta\hat{b}^\dagger$, $\delta\hat{a}^\dagger$, i.e., $2D_{AA} = 2\kappa M_s$, $2D_{BA} = -iG_1/2$, $2D_{AA^*} = 2\kappa(N_s + 1)$, and $2D_{BB^*} = 2\gamma_m(n_t + 1)$. For the convenience of calculation, we define the dimensionless amplitude and phase fluctuations of the cavity field as $X = (A + A^*)/\sqrt{2}$ and $Y = i(A^* - A)/\sqrt{2}$. The corresponding noise functions are, $F_x(t) = (F_A + F_A^*)/\sqrt{2}$ and $F_y(t) = (F_A - F_A^*)/\sqrt{2}i$, respectively. Similarly, the position and momentum fluctuations of the mechanical oscillator are, $q = (B + B^*)/\sqrt{2}$ and $p = (B - B^*)/\sqrt{2}i$, respectively. The corresponding thermal noise terms read, $\xi_q(t) = (F_B + F_B^*)/\sqrt{2}$ and $\xi_p(t) = i(F_B^* - F_B)/\sqrt{2}$, respectively. Further, by introducing the vectors of continuous-variable quadratures $x = (q, X)^T$ and $y = (p, Y)^T$, and the corresponding vectors of noises $f_x(t) = (\xi_q(t), F_x(t))^T$ and $f_y(t) = (\xi_p(t), F_y(t))^T$, the linearized c-number Langevin equation (4) can be written in the following matrix form:

$$\dot{x} = -K_1 x + \Phi_1 y + f_x(t),$$
$$\dot{y} = -K_1 y - \Phi_2 x + f_y(t), \tag{6}$$

where the coefficient matrices $K_1 = (\gamma_m, 0; 0, \kappa)$, $\Phi_1 = (\omega_m, 0; 0, \Delta)$ and $\Phi_2 = (\omega_m, -G; -G, \Delta)$ with $G = 2G_1$. The nonvanishing c-number correlation functions for these noises are given as

$$\langle \xi_{q,p}(t)\xi_{q,p}(t') \rangle = 2\gamma_m(n_t + 1)\delta(t - t'),$$
$$\langle F_{x,y}(t)F_{x,y}(t') \rangle = 2\kappa N_{+,-}\delta(t - t'),$$
$$\langle \xi_q(t)F_y(t') \rangle = -G/4\delta(t - t'),$$
$$\langle \xi_p(t)F_x(t') \rangle = -G/4\delta(t - t'),$$
$$\langle F_x(t)F_y(t') \rangle = 2\kappa M_s^I \delta(t - t'), \tag{7}$$

where $N_\pm = N_s + 1 \pm M_s^R$, $M_s^R = (M_s + M_s^*)/2$ and $M_s^I = (M_s - M_s^*)/(2i)$.

III. SECOND MOMENT AT FIXED TIME DURATION AND STEADY-STATE DISTRIBUTION

To study the thermo-phonon transport in a nonequilibrium steady state and the Berry-phase-like effect of the thermo-phonon transfer in the optomechanical system, we need evaluate second moments at a fixed time duration τ. By using the finite time Fourier transform [70]

$$h(\omega_n) = \frac{1}{\tau}\int_0^\tau h(t)e^{-i\omega_n t}dt,$$
$$h(t) = \sum_{n=-\infty}^{n=\infty} h(\omega_n)e^{i\omega_n t}, \tag{8}$$

where $\omega_n = 2\pi n/\tau$, one can write Eq. (6) in the Fourier basis as

$$x(\omega_n) = H[\Phi_1 f_y(\omega_n) + Kf_x(\omega_n)] - \frac{H}{\tau}(K\Delta X_\tau + \Phi_1 \Delta Y_\tau),$$
$$y(\omega_n) = Mf_y(\omega_n) - Nf_x(\omega_n) + \frac{1}{\tau}(N\Delta X_\tau - M\Delta Y_\tau), \tag{9}$$

where $K = K_1 + I \times i\omega_n$, $H = (K^2 + \Phi_1\Phi_2)^{-1}$, $M = K^{-1}(I - \Phi_2 H\Phi_1)$, $N = K^{-1}\Phi_2 HK$; $\Delta X_\tau = x(\tau) - x(0)$ and $\Delta Y_\tau = y(\tau) - y(0)$; I is the identity matrix.

By using the above expressions of the vectors $x(\omega_n)$ and $y(\omega_n)$ in the frequency domain, the quadratures of the continuous-variable quantum system, i.e., p, Y, q, and X, are

$$p(\omega_n) = -N_{11}\xi_q(\omega_n) + M_{11}\xi_p(\omega_n) - N_{12}F_x(\omega_n)$$
$$+ M_{12}F_y(\omega_n) + \frac{1}{\tau}q_5^T\Delta U(\tau), \tag{10}$$

$$Y(\omega_n) = -N_{21}\xi_q(\omega_n) + M_{21}\xi_p(\omega_n) - N_{22}F_x(\omega_n)$$
$$+ M_{11}F_y(\omega_n) + \frac{1}{\tau}q_6^T\Delta U(\tau), \tag{11}$$

$$q(\omega_n) = (HK)_{11}\xi_q(\omega_n) + (H\Phi_1)_{11}\xi_p(\omega_n) + (HK)_{12}F_x(\omega_n)$$
$$+ (H\Phi_1)_{12}F_y(\omega_n) - \frac{1}{\tau}q_7^T\Delta U(\tau), \tag{12}$$

$$X(\omega_n) = (HK)_{21}\xi_q(\omega_n) + (H\Phi_1)_{21}\xi_p(\omega_n) + (HK)_{22}F_x(\omega_n)$$
$$+ (H\Phi_1)_{22}F_y(\omega_n) - \frac{1}{\tau}q_8^T\Delta U(\tau), \tag{13}$$

where

$$q_5^T = [N_{11}, N_{12}, -M_{11}, -N_{12}], \tag{14}$$

$$q_6^T = [N_{21}, N_{22}, -M_{21}, M_{22}], \tag{15}$$

$$q_7^T = [(HK)_{11}, (HK)_{12}, (H\Phi_1)_{11}, (H\Phi_1)_{12}], \tag{16}$$

$$q_8^T = [(HK)_{21}, (HK)_{22}, (H\Phi_1)_{21}, (H\Phi_1)_{22}], \tag{17}$$

and $\Delta U(\tau) = (\Delta X_\tau^T, \Delta Y_\tau^T)^T$; N_{ij} with $i, j = 1, 2, 3, 4$ denotes the element of the ith row and the jth column of matrix N and so on.

In order to calculate the value of ΔU, a specific expression for row vector $U^T(\tau) = (x^T(\tau), y^T(\tau))$ is needed. By using Fourier series representation for $x(t)$ and $y(t)$, the value at time τ can be obtained from the Fourier series by setting

$t = \tau - \epsilon$, $\epsilon > 0$ and taking the limit $\epsilon \to 0$. Therefore we calculate $U^T(\tau)$ as

$$U^T(\tau) = \lim_{\epsilon \to 0} \sum_{n=-\infty}^{n=\infty} e^{-i\omega_n \epsilon} [x^T(\omega_n), y^T(\omega_n)]. \quad (18)$$

Here we have used $\omega_n = 2\pi n/\tau$. In the large time limit $\tau \to \infty$, the above given summation can be converted into integration over ω. Substituting Eq. (9) into Eq. (18), we have [70,72]

$$\lim_{\epsilon \to 0} \int_{-\infty}^{\infty} \frac{d\omega}{2\pi} e^{-i\omega \epsilon} \left[\Delta X_\tau^T K^T + \Delta Y_\tau^T \Phi_1^T \right] \frac{H^T}{\tau} \to 0, \quad (19)$$

$$\lim_{\epsilon \to 0} \int_{-\infty}^{\infty} \frac{d\omega}{2\pi} e^{-i\omega \epsilon} \left[\Delta X_\tau^T \frac{N^T}{\tau} - \Delta Y_\tau^T \frac{M^T}{\tau} \right] \to 0, \quad (20)$$

because all the poles of the integrand lie in the upper half of the complex ω plane. Therefore $U(\tau)$ becomes

$$U^T(\tau) = \lim_{\epsilon \to 0} \sum_{n=-\infty}^{n=\infty} e^{-i\omega_n \epsilon} \big[\xi_q(\omega_n) q_1^T + F_x(\omega_n) q_2^T$$
$$+ \xi_p(\omega_n) q_3^T + F_y(\omega_n) q_4^T \big], \quad (21)$$

where

$$q_1^T = [(HK)_{11}, (HK)_{21}, -N_{11}, -N_{21}], \quad (22)$$

$$q_2^T = [(HK)_{12}, (HK)_{22}, -N_{12}, -N_{22}], \quad (23)$$

$$q_3^T = [(H\Phi_1)_{11}, (H\Phi_1)_{21}, M_{11}, M_{21}], \quad (24)$$

$$q_4^T = [(H\Phi_1)_{12}, (H\Phi_1)_{22}, M_{12}, M_{22}]. \quad (25)$$

Consequently, using the c-number correlation functions for the noises $\xi_{q,p}(t)$ and $F_{x,y}(t)$, we can easily find out the mean $\langle U(\tau) \rangle = 0$ and the correlations of $U(\tau)$

$$\langle U(\tau) U^T(\tau) \rangle = \int_{-\infty}^{\infty} \frac{d\omega}{2\pi} \{ \langle \xi_q \xi_q^* \rangle q_1 q_1^\dagger + \langle F_x F_x^* \rangle q_2 q_2^\dagger$$
$$+ \langle \xi_p \xi_p^* \rangle q_3 q_3^\dagger + \langle F_y F_y^* \rangle q_4 q_4^\dagger + \langle \xi_q F_y^* \rangle q_1 q_4^\dagger$$
$$+ \langle F_y \xi_q^* \rangle q_4 q_1^\dagger + \langle \xi_p F_x^* \rangle q_3 q_2^\dagger + \langle F_x \xi_p^* \rangle q_2 q_3^\dagger$$
$$+ \langle F_x F_y^* \rangle q_2 q_4^\dagger + \langle F_y F_x^* \rangle q_4 q_2^\dagger \}. \quad (26)$$

Here we write $\xi_{q,p}^*(\omega_n) = \xi_{q,p}(-\omega_n)$ and $F_{x,y}^*(\omega_n) = F_{x,y}(-\omega_n)$. In the present model, U is a linear function of Gaussian noises, thus the steady state distribution can be written in terms of the mean and the correlations of $U(\tau)$ as

$$P(U, \tau \to \infty | U_0) = P_{ss}(U) = \frac{e^{-\frac{1}{2} U^T v^{-1} U}}{\sqrt{(2\pi)^4 \det v}} \quad (27)$$

with the matrix element $v_{ij} = \langle U_i(\tau) U_j^T(\tau) \rangle$.

IV. STEADY-STATE THERMO-PHONON FLUX

Now we evaluate the fluctuating term in $N_{p0}(\tau)$, i.e., $\hat{N}_{p1}(\tau) = \int_0^\tau [\hat{\xi}_p(t) - \gamma_m \delta \hat{p}(t)] \delta \hat{p}(t) dt$, using c-number quadrature $p(t)$ in Eq. (6), which depends on the initial conditions of the system $U_0 = U(t = 0)$ with $U^T = (x^T, y^T)$ and the noise trajectory $\{\xi_p(t) : 0 \leqslant t \leqslant \tau\}$ in any particular

realization. To achieve this goal, we introduce the probability distribution of $N_p(\tau) = \int_0^\tau [\xi_p(t) - \gamma_m p(t)] p(t) dt$ with $\langle N_p \rangle \equiv \langle \hat{N}_{p1} \rangle$, $P(N_p, \tau)$, and the corresponding characteristic function for the thermo-phonon counting field λ, $Z(\lambda) = \langle e^{-\lambda N_p} \rangle$, where $\langle \cdots \rangle$ denotes an average over initial configurations as well as over different paths [70,72]. In general, for a given initial configuration U_0 and a given final configuration U in time τ, the characteristic function can be written as $Z(\lambda, U, \tau | U_0) = \langle e^{-\lambda N_p} \rangle_{U_0, U}$, which satisfies a FP type of equation [70]:

$$[\partial_\tau - L_\lambda] Z(\lambda, U, \tau | U_0) = 0 \quad (28)$$

with the initial condition $Z(\lambda, U, \tau | U_0) = \delta(U - U_0)$, where L_λ is the FP operator and reads

$$L_\lambda = \left[\frac{\partial H_e}{\partial q} \frac{\partial}{\partial p} - \frac{\partial H_e}{\partial p} \frac{\partial}{\partial q} \right] + \left[\frac{\partial H_e}{\partial X} \frac{\partial}{\partial Y} - \frac{\partial H_e}{\partial Y} \frac{\partial}{\partial X} \right]$$
$$+ \gamma_m \left(\frac{\partial}{\partial q} q + \frac{\partial}{\partial p} p \right) + \kappa \left(\frac{\partial}{\partial X} X + \frac{\partial}{\partial Y} Y \right)$$
$$+ 2\lambda \gamma_m (n_t + 1) \frac{\partial}{\partial p} p + \kappa N_+ \frac{\partial}{\partial X^2} + \kappa N_- \frac{\partial}{\partial Y^2}$$
$$+ \gamma_m (n_t + 1) \left(\lambda^2 p^2 + \frac{\partial}{\partial q^2} + \frac{\partial}{\partial p^2} \right)$$
$$+ \lambda [\gamma_m p^2 - \gamma_m (n_t + 1)] + \kappa M_s^I \left(\frac{\partial^2}{\partial X \partial Y} + \frac{\partial^2}{\partial Y \partial X} \right)$$
$$+ \frac{G}{8} \left(\frac{\partial^2}{\partial q \partial Y} + \frac{\partial^2}{\partial Y \partial q} \right) + \frac{G}{8} \left(\frac{\partial^2}{\partial p \partial X} + \frac{\partial^2}{\partial X \partial p} \right), \quad (29)$$

with $H_e = \frac{\omega_m}{2}(p^2 + q^2) + \frac{\Delta}{2}(X^2 + Y^2) - GXq$ is the effective Hamiltonian of the coupled optomechanical system.

The formal solution of the above differential equation can be expressed in the eigenbases of the FP operator L_λ and the large τ behavior is dominated by the term having the largest eigenvalue $\mu(\lambda)$ of the operator L_λ, i.e., $Z(\lambda, U, \tau | U_0) = e^{(\tau/\tau_\gamma)\mu(\lambda)} \Pi(U_0, \lambda) \Psi(U, \lambda)$, where $\tau_\gamma = 1/\gamma_m$ is the viscous relaxation time of the system [72]. $\Pi(U_0, \lambda)$ and $\Psi(U, \lambda)$ are, respectively, the left and right eigenfunctions corresponding to the largest eigenvalue, which satisfy the orthonormality condition $\int dU \Psi(U, \lambda) \Pi(U, \lambda) = 1$. It is noted that for $\lambda = 0$, $Z(0, U, \tau | U_0) = P(U, \tau | U_0)$ is the joint distribution of U at time τ starting from U_0. Consequently, in the large time limit, a unique nonequilibrium steady state can be calculated from $Z(0, U, \tau \to \infty | U_0) = P_{ss}(U) = \Psi(U)$ [see Eq. (27)], which implies that $\mu = 0$ and $\Pi(U_0, 0) = 1$.

Using the restricted characteristic function in the large τ limit and the steady-state distribution P_{ss}, we have $Z(\lambda) = g(\lambda) e^{(\tau/\tau_\gamma)\mu(\lambda)}$ with $g(\lambda) = \int dU_0 \Psi(U_0, 0) \Pi(U_0, \lambda) \int dU \Psi(U, \lambda)$. For large τ the prefactor $g(\lambda)$ can usually be ignored [70,72]. Then, the eigenvalue $\mu(\lambda)$ can be used to describe the cummulant generating function (CGF) of the optomechanical system, which is given by $\mathcal{G}(\lambda) = \lim_{\tau \to \infty} \ln Z(\lambda)/\tau$ and contains information about the first-order cumulant of thermo-phonon current fluctuations, such as, $J_1(\tau) = \lim_{\tau \to \infty} \langle N_p \rangle / \tau = -\partial G(\lambda)/\partial \lambda |_{\lambda=0}$ [65,70]. Consequently, the total average

thermo-phonon flux $J_p = \lim_{\tau \to \infty} \langle N_{p0}(\tau) \rangle / \tau$ becomes

$$J_p = -\gamma_m p_s^2 - \tau_\gamma^{-1} \partial_\lambda \mu(\lambda)|_{\lambda=0}. \quad (30)$$

In general, the largest eigenvalue and the corresponding eigenfunctions are difficult to attain by solving the FP equation. Nevertheless, these functions can still be evaluated by a technique developed in Ref. [70]. In the following, we derive the largest eigenvalue and corresponding eigenvectors of the Fokker-Planck equation. By using the above finite time Fourier transform, we now write $N_p(\tau) = \int_0^\tau [\xi_p(t) - \gamma_m p(t)] p(t) dt$ as

$$N_p(\tau) = \frac{1}{2} \tau \sum_{n=-\infty}^{n=\infty} [\xi_p(\omega_n) p(-\omega_n) + \xi_p(-\omega_n) p(\omega_n) - 2\gamma_m p(\omega_n) p(-\omega_n)]. \quad (31)$$

Substituting $p(\omega_n)$ from Eq. (10) into the above equation, we get

$$N_p(\tau) = \frac{1}{2} \tau \sum_{n=-\infty}^{n=\infty} \left\{ [\xi_p(\omega_n) B_- + \xi_p(-\omega_n) A_+ - 2\gamma_m A_+ B_-] \right.$$
$$+ \left[\xi_p(\omega_n) \frac{q_5^\dagger}{\tau} \Delta U + \xi_p(-\omega_n) \frac{q_5^T}{\tau} \Delta U - 2\gamma_m A_+ \frac{q_5^\dagger}{\tau} \Delta U \right.$$
$$\left. \left. - 2\gamma_m B_- \frac{q_5^T}{\tau} \Delta U - 2\gamma_m \frac{\Delta U^T q_5 q_5^\dagger \Delta U}{\tau^2} \right] \right\}, \quad (32)$$

where $A_+ = -N_{11}\xi_q(\omega_n) + M_{11}\xi_p(\omega_n) - N_{12}F_x(\omega_n) + M_{12}F_y(\omega_n)$ and $B_- = M_{11}^*\xi_p(-\omega_n) - N_{11}^*\xi_q(-\omega_n) - N_{12}^*F_x(-\omega_n) + M_{12}^*F_y(-\omega_n)$. Further, the restricted characteristic function for N_p can be written as [70,72]

$$Z(\lambda, U, \tau | U_0) = \langle e^{-\lambda N_p} \delta(U - U(\tau)) \rangle |_{U,U_0}$$
$$= \int \frac{d^4\sigma}{(2\pi)^4} e^{i\sigma^T U} \langle e^{E(\tau)} \rangle |_{U,U_0}, \quad (33)$$

where we replace the δ-function by the integral representations $\delta(U - U(\tau)) = \int d^4\sigma/(2\pi)^4 e^{i\sigma^T(U-U(\tau))}$ with $\sigma^T = (\sigma_1, \sigma_2, \sigma_3, \sigma_4)$. Also $E(\tau) = -\lambda N_p(\tau) - i\sigma^T U(\tau)$, which can be written as by using Eqs. (21) and (32),

$$E(\tau) = \sum_{n=1}^{n=\infty} \left[-\lambda\tau \zeta_n^T \Upsilon_n \zeta_n^* + \zeta_n^T \beta_n + \beta_{-n}^T \zeta_n^* + \frac{2\gamma_m}{\tau} |f_n|^2 \right]$$
$$- \frac{\lambda\tau}{2} \zeta_0^T \Upsilon_0 \zeta_0^* + \zeta_0^T \beta_0 + \frac{\gamma_m}{\tau} |f_0|^2, \quad (34)$$

where $f_n = q_5^T \Delta U$ and the row vector $\zeta_n^T = (\xi_q(\omega_n), F_x(\omega_n), \xi_p(\omega_n), F_y(\omega_n))$. The matrix Υ_n is

$$\frac{\Upsilon_n}{2\gamma_m} = \begin{pmatrix} -|N_{11}|^2 & -N_{11}N_{12}^* & N_{11}\Upsilon_{11} & N_{11}M_{12}^* \\ -N_{11}^*N_{12} & -|N_{12}|^2 & N_{12}\Upsilon_{11} & N_{12}M_{12}^* \\ N_{11}^*\Upsilon_{11}^* & N_{12}^*\Upsilon_{11}^* & \Upsilon_{33} & -M_{12}^*\Upsilon_{11}^* \\ N_{11}^*M_{12} & N_{12}^*M_{12} & -M_{12}\Upsilon_{11} & -|M_{12}|^2 \end{pmatrix} \quad (35)$$

with $\Upsilon_{33} = M_{11}^*/(2\gamma_m) - M_{11}\Upsilon_{11}$ and $\Upsilon_{11} = [M_{11}^* - 1/(2\gamma_m)]$. The column vector β_n is given by

$$\beta_n = \lambda \begin{pmatrix} C_{11}^T \Delta U \\ C_{21}^T \Delta U \\ C_{31}^T \Delta U \\ C_{41}^T \Delta U \end{pmatrix} - i e^{-i\omega_n \epsilon} \begin{pmatrix} q_1^T \sigma \\ q_2^T \sigma \\ q_3^T \sigma \\ q_4^T \sigma \end{pmatrix}, \quad (36)$$

where $C_{11}^T = -2\gamma_m N_{11} q_5^\dagger$, $C_{21}^T = -2\gamma_m N_{12} q_5^\dagger$, $C_{31}^T = [2\gamma_m M_{11} - 1] q_5^\dagger$, and $C_{41}^T = 2\gamma_m M_{12} q_5^\dagger$. Therefore, we can evaluate the average ($\langle e^{E(\tau)} \rangle_{U,U_0}$) with respect to the joint Gaussian distribution of thermal and vacuum noises, ζ_n,

$$\langle e^{E(\tau)} \rangle_{U,U_0} = \left\langle \exp\left[-\frac{\lambda\tau}{2} \zeta_0^T \Upsilon_0 \zeta_0^* + \zeta_0^T \beta_0 + \frac{\gamma_m}{\tau} |f_0|^2 \right] \right\rangle$$
$$\times \prod_{n=1}^{n=\infty} \left\langle \exp\left[-\lambda\tau \zeta_n^T \Upsilon_n \zeta_n^* + \zeta_n^T \beta_n + \beta_{-n}^T \zeta_n^* \right. \right.$$
$$\left. \left. + \frac{2\gamma_m}{\tau} |f_n|^2 \right] \right\rangle, \quad (37)$$

In the above Eq. (37), for $n \geqslant 1$, the Gaussian distribution is [70]

$$P(\zeta_n) = \frac{\exp(-\zeta_n^T D^{-1} \zeta_n^*)}{\pi^4 \det D}, \quad (38)$$

and for $n = 0$, the noise ζ_0 has the following Gaussian distribution:

$$P(\zeta_0) = \frac{\exp(-\frac{1}{2}\zeta_0^T D^{-1} \zeta_0)}{\sqrt{(2\pi)^4 \det D}}, \quad (39)$$

where D is the 4×4 noise matrix

$$D = \frac{1}{\tau} \begin{pmatrix} 2\gamma_m(n_t + 1) & 0 & 0 & -G/4 \\ 0 & 2\kappa N_+ & -G/4 & 2\kappa M_s^I \\ 0 & -G/4 & 2\gamma_m(n_t + 1) & 0 \\ -G/4 & 2\kappa M_s^I & 0 & 2\kappa N_- \end{pmatrix}. \quad (40)$$

Using Eqs. (37)–(39) and complex Gaussian integration [70], we get

$$\langle e^{E(\tau)} \rangle_{U,U_0} = \exp\left(-\frac{1}{2} \sum_{n=-\infty}^{n=\infty} \ln[\det(I + \lambda\tau D \Upsilon_n)] \right)$$
$$\times \exp\left(\sum_{n=-\infty}^{n=\infty} \left[\frac{1}{2} \beta_{-n}^T \Lambda \beta_n + \frac{\lambda\gamma_m}{\tau} |f_n|^2 \right] \right) \quad (41)$$

with $\Lambda = (D^{-1} + \lambda\tau \Upsilon_n)^{-1}$. In the large time limit $\tau \to \infty$, we may replace all the summations over n by integration over ω. Then, Eq. (41) can be written as

$$\langle e^{E(\tau)} \rangle_{U,U_0} \approx \exp\left[\frac{\tau}{\tau_\gamma} \mu(\lambda) \right] \exp\left(-\frac{1}{2} \sigma^T H_1 \sigma + i\Delta U^T H_2 \sigma \right.$$
$$\left. + \frac{1}{2} \Delta U^T H_3 \Delta U \right), \quad (42)$$

where

$$\mu(\lambda) = -\frac{\tau_\gamma}{4\pi} \int_{-\infty}^{\infty} d\omega \ln[\det(I + \lambda\tau D\Upsilon_n)], \qquad (43)$$

$$H_1(\lambda) = \frac{\tau}{2\pi} \int_{-\infty}^{\infty} d\omega \rho^T (D^{-1} + \lambda\tau\Upsilon_n)^{-1}\phi, \qquad (44)$$

$$H_2(\lambda) = \lim_{\epsilon \to 0} \frac{-\tau}{2\pi} \int_{-\infty}^{\infty} d\omega e^{-i\omega\epsilon} a_1^\dagger (D^{-1} + \lambda\tau\Upsilon_n)^{-1}\phi, \qquad (45)$$

$$H_3(\lambda) = \frac{\tau}{2\pi} \int_{-\infty}^{\infty} d\omega \left[a_1^T (D^{-1} + \lambda\tau\Upsilon_n)^{-1}a_2 + \frac{\lambda\gamma_m q_5 q_5^\dagger}{\tau} \right] \qquad (46)$$

with $\rho^T = (q_1^*, q_2^*, q_3^*, q_4^*)$ and $a_1^T = \lambda(d_{11}, d_{12}, d_{13}, d_{14})$ with $d_{11} = 2\gamma_m N_{11}^* q_5$, $d_{12} = -2\gamma_m N_{12}^* q_5$, $d_{13} = [2\gamma_m M_{11}^* - 1]q_5$, $d_{14} = 2\gamma_m M_{12}^* q_5$; and

$$\phi = \begin{pmatrix} q_1^T \\ q_2^T \\ q_3^T \\ q_4^T \end{pmatrix}, \quad a_2 = \lambda \begin{pmatrix} C_{11}^T \\ C_{21}^T \\ C_{31}^T \\ C_{41}^T \end{pmatrix}. \qquad (47)$$

Finally, substituting the expression for $\langle e^{E(\tau)} \rangle_{U,U_0}$ from Eq. (42) into Eq. (33) and performing the Gaussian integration over σ, the restricted characteristic function for N_p becomes

$$Z(\lambda, U, \tau|U_0) \approx \exp\left[\frac{\tau}{\tau_\gamma}\mu(\lambda) \right] \frac{\exp\left(\frac{1}{2}\Delta U^T H_3 \Delta U \right)}{\sqrt{(2\pi)^4 \det H_1(\lambda)}} \exp$$

$$\times \left[-\frac{1}{2}(U^T + \Delta U^T H_2) H_1^{-1}(U + H_2^T \Delta U) \right]. \qquad (48)$$

It is noted that the initial and the final variables in Eq. (48) must factorize in terms of the large τ behavior of the restricted characteristic function $Z(\lambda, U, \tau|U_0)$. Thus, we have

$$\left(H_3 - H_2 H_1^{-1} H_2^T - H_1^{-1} H_2^T \right)$$

$$+ \left(H_3 - H_2 H_1^{-1} H_2^T - H_2 H_1^{-1} \right)^T = 0. \qquad (49)$$

Using Eq. (49), the restricted characteristic function for N_p is expressed as

$$Z(\lambda, U, \tau|U_0) \approx \exp\left[\frac{\tau}{\tau_\gamma}\mu(\lambda) \right] \exp\left[-\frac{1}{2}U_0^T R_2(\lambda) U_0 \right]$$

$$\times \frac{\exp\left[-\frac{1}{2}U^T R_1(\lambda) U \right]}{\sqrt{(2\pi)^4 \det H_1(\lambda)}}, \qquad (50)$$

where $R_1(\lambda) = H_1^{-1}(\lambda) + H_1^{-1}(\lambda)H_2^T(\lambda)$ and $R_2(\lambda) = -H_1^{-1}(\lambda)H_2^T(\lambda)$. Comparing restricted characteristic function $Z(\lambda, U, \tau|U_0) = e^{(\tau/\tau_\gamma)\mu(\lambda)}\Pi(U_0, \lambda)\Psi(U, \lambda)$ and (50), the right and left eigenvectors of the Fokker-Planck operator L_λ, $\Psi(U, \lambda)$ and $\Pi(U_0, \lambda)$ can be identified:

$$\Psi(U, \lambda) = \frac{\exp\left[-\frac{1}{2}U^T R_1(\lambda) U \right]}{\sqrt{(2\pi)^4 \det H_1(\lambda)}}, \qquad (51)$$

$$\Pi(U_0, \lambda) = \exp\left[-\frac{1}{2}U_0^T R_2(\lambda) U_0 \right], \qquad (52)$$

which correspond to the eigenvalue $\mu(\lambda)$ and satisfy the orthonormality condition $\int dU \Psi(U, \lambda)\Pi(U, \lambda) = 1$. Using
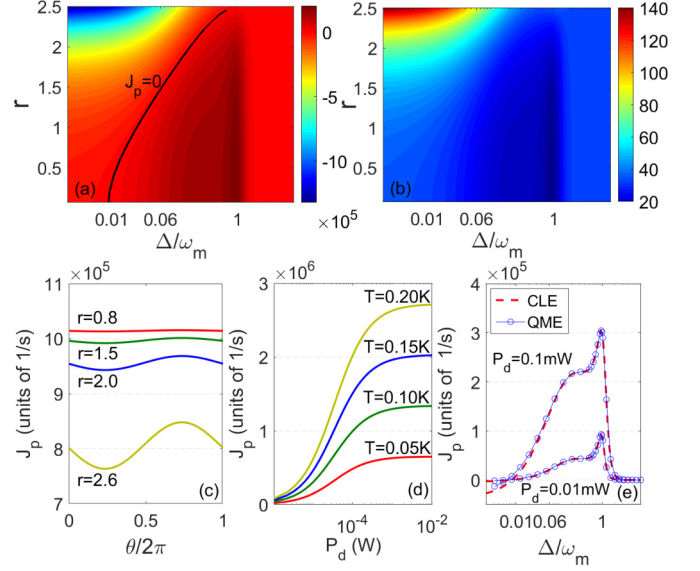

FIG. 2. The contour of (a) J_p and (b) n_{ph}^{eff} vs Δ/ω_m and r, where the black line denotes the transition of J_p from positive to negative. J_p as a function of (c) θ and (d) P_d with different r's or T's. (e) J_p as a function of Δ/ω_m. The red dash lines depict the analytical results [Eq. (53)] from CGF, while the blue lines with circles mark the simulation results from the exact QME approach. Feasible experimental parameters are [6] $\lambda_d = 810$ nm, $L = 1$ mm, $m = 50$ ng, $\omega_m = 2\pi \times 10$ MHz, $\kappa = 0.2\omega_m$, $\gamma_m = 10^{-4}\omega_m$. (a) and (b) $\theta = \pi/2$, $P_d = 0.1$ mW and $T = 0.02$ K; (c) $\Delta = \omega_m$, $P_d = 0.1$ mW and $T = 0.1$ K; (d) $\Delta = \omega_m$, $\theta = \pi/2$ and $r = 1.5$. (e) $r = 0.5$, $\theta = \pi/2$, and $T = 0.03$ K.

Eqs. (30) and (43), the thermo-phonon flux J_p can be written as

$$J_p = -\gamma_m p_s^2 + \frac{1}{4\pi} \int_{-\infty}^{\infty} d\omega [\text{Tr}(D_0 \Upsilon_n(\omega))], \qquad (53)$$

which describes a general formula of the thermo-phonon transfer between the two-mode subsystem and its bath. Here $D_0 = D\tau$.

Figure 2(a) show the flux J_p as a function of the normalized detuning Δ/ω_m and the squeezing strength r. It is found from Fig. 2(a) that the maximum of J_p appears at the optimal detuning $\Delta = \omega_m$ with different r's, which originates from the most efficient energy transfer from the mechanical to the optical mode marked by the black ring in Fig. 1(b) when the beam splitter interaction between them, i.e., $\delta\hat{a}^\dagger\delta\hat{b} + \delta\hat{a}\delta\hat{b}^\dagger$ in H_L is in resonance. The maximum can help identify the optimal cooling of a mechanical motion, which appears identically at $\Delta \approx \omega_m$ and is evaluated by counting the effective phonon numbers of the vibration fluctuations, i.e., $n_{ph}^{eff} = (v_{11} + v_{33} - 1)/2$ with v_{ij} being the second moments in Eq. (27), shown in Fig. 2(b). It is noted that the flux $J_p \to 0$ as $\Delta \gg \omega_m$ because G_1 becomes very small, which acts as a coupling channel for the energy transfer. Furthermore, the increasing noise correlation enhances the effective temperature of the optical mode and therefore changes the nonequilibrium characteristics of the system, so that the flux switches from positive to negative. The energy transfer from the squeezed vacuum bath to the mechanical thermal bath can be seen as a result of the

transfer of squeezing from light to mechanical oscillator, which is best under the condition of optomechanical cooling [73]. Figure 2(c) displays a periodic variation of J_p with θ and Fig. 2(d) shows that an increase of P_d or T leads to an increase of J_p, due to the increment of G_1 or thermal noise strength. In Fig. 2(e), we evaluate the steady-state flux with the method of QME (see Appendix) and shows that the analytical result [Eq. (53)] from CGF are well fitted with the exact results from QME when G_1 is weak, i.e., the driving power is relatively small or the detuning Δ is relatively large.

V. OPTOMECHANICAL BERRY-PHASE-LIKE EFFECT

We now assume that the optomechanical system is already at its steady state. And then, a cyclic time-dependent modulation is imposed adiabatically on the system. In this case, the CGF will gain an additional term, resulting in a geometric thermo-phonon transport originating from the nontrivial curvature in the parameter space of the system [76,81], which can be studied in terms of the instantaneous eigenvalue $\mu(\lambda, t)$ and the left and right eigenvectors ($\Pi(U, \lambda, t)$ and $\Psi(U, \lambda, t)$) as well as the steady-state values, i.e., $p_s(t)$. Following Refs. [65,76,81], the CGF for adiabatically driven system is composed of two parts, the dynamical part and the additional geometric one: $\mathcal{G}(\lambda) = \mathcal{G}_{\mathrm{dyn}} + \mathcal{G}_{\mathrm{geom}}$, where the dynamical contribution

$$\mathcal{G}_{\mathrm{dyn}} = -\tau_\gamma^{-1} T_p^{-1} \int_0^{T_p} dt\, \mu(\lambda, t), \tag{54}$$

which survives whenever the system's parameters are static or experience single or multiple modulations. Here, T_p is the modulation period. The geometric contribution of the thermophonon transport $\mathcal{G}_{\mathrm{geom}}$ is [65]

$$\mathcal{G}_{\mathrm{geom}} = -\frac{1}{T_p} \int_0^{T_p} dt \int_{-\infty}^{\infty} dU\, \Pi(U, \lambda, t)\dot{\Psi}(U, \lambda, t), \tag{55}$$

which is called as the optomechanical Berry-phase like and generated when at least two parameters are modulated temporally. In the present optomechanical model, we can modulate simultaneously the parameters M_s^I and M_s^R related to the injected vacuum noise [73,75]. In the case of periodically driving pairs $(u_1(t), u_2(t))$, the geometric contribution $\mathcal{G}_{\mathrm{geom}}$, can be expressed as

$$\mathcal{G}_{\mathrm{geom}} = -\frac{1}{T_p}\left[\oint P_u du_1 + \oint Q_u du_2 \right], \tag{56}$$

where

$$P_u = \int_{-\infty}^{\infty} dU\, \Pi(U, \lambda, u_1, u_2, t)\frac{\partial \Psi}{\partial u_1}, \tag{57}$$

$$Q_u = \int_{-\infty}^{\infty} dU\, \Pi(U, \lambda, u_1, u_2, t)\frac{\partial \Psi}{\partial u_2}. \tag{58}$$

Using Eqs. (51) and (52) as well as the multidimensional integration integration

$$\int dz [z^T G_n z] \exp\left[-\frac{1}{2} z^T L_n z\right] = \sqrt{\frac{(2\pi)^N}{\det L_n}} \mathrm{Tr}[G_n L_n^{-1}], \tag{59}$$

where $z = [z_1, z_2, \ldots, z_N]^T$, G_n and L_n are nonsingular matrices, we get

$$P_u = -\frac{1}{2}\mathrm{Tr}\left[\frac{\partial R_1(\lambda)}{\partial u_1} H_1(\lambda)\right] - \frac{1}{2}\mathrm{Tr}\left[H_1^{-1}(\lambda)\frac{\partial H_1(\lambda)}{\partial u_1}\right],$$

$$Q_u = -\frac{1}{2}\mathrm{Tr}\left[\frac{\partial R_1(\lambda)}{\partial u_2} H_1(\lambda)\right] - \frac{1}{2}\mathrm{Tr}\left[H_1^{-1}(\lambda)\frac{\partial H_1(\lambda)}{\partial u_2}\right]. \tag{60}$$

Further, using Stokes theorem, we have

$$\mathcal{G}_{\mathrm{geom}} = \frac{1}{T_p} \iint_{u_1 u_2} du_1 du_2\, \Xi_{u_1 u_2}(\lambda), \tag{61}$$

where the subscript $u_1 u_2$ denotes the integral area enclosed by the modulation contour of $(u_1(t), u_2(t))$ and

$$\Xi_{u_1 u_2}(\lambda) = \frac{1}{2}\mathrm{Tr}\left[\frac{\partial H_1(\lambda)}{\partial u_2}\frac{\partial R_2(\lambda)}{\partial u_1} - \frac{\partial H_1(\lambda)}{\partial u_1}\frac{\partial R_2(\lambda)}{\partial u_2}\right] \tag{62}$$

is the so-called Berry curvature, which is an analog of a Berry phase in quantum mechanics and generated when at least two parameters are modulated temporally, i.e., periodically driven pairs $(u_1(t), u_2(t))$ [62]. Obviously, this quantity in the optomechanical continuous-variable system has a form similar to the Berry curvature in quantum mechanics and therefore can be identified with Berry curvature [65], which is independent of the modulation rate and a purely geometric property. It is noted that the functions $H_1(\lambda)$ and $R_2(\lambda)$ in the above curvature are no longer the right and left eigenvectors of the Fokker-Planck operator, different from the curvature for continuous function space of an overdamped coupled oscillator system [65]. Even so, we see that the right and left eigenvectors of the Fokker-Planck operator [Eqs. (51) and (52)] are always associated with the functions $H_1(\lambda)$ and $R_2(\lambda)$, respectively.

It is noted that Eq. (6) can describe directly the dynamical behavior of a classical coupled oscillator system in contact with different dissipative sources with large classical fluctuations. Therefore, the curvature obtained here can be applied not only to the current quantum optomechanical system, but also to the underdamped coupled oscillator system with nonzero inertia. In particular, we can straightforwardly extend the present method to study the thermal noise energy harvesting and rectification of multimode coupled quantum systems or classical oscillator chains with inertial terms by increasing properly the dimensions of the relevant matrices in Eq. (6). Consequently, the curvature in Eq. (62) is universal, whose form remains unchanged except for the increment of the dimensions of the matrices $H_1(\lambda)$ and $R_2(\lambda)$ in multimode oscillator subsystems.

According to the first cumulant of thermo-phonon fluctuations, in the presence of the modulation the average flux becomes $J_p = J_{\mathrm{dyn}} + J_{\mathrm{geom}}$, with $J_{\mathrm{dyn}} = T_p^{-1} \int_0^{T_p} dt[-\gamma_m p_s^2(t) - \tau_\gamma^{-1}\partial\mu(\lambda, t)/\partial\lambda|_{\lambda=0}]$ being the dynamical thermo-phonon flux and $J_{\mathrm{geom}} = T_p^{-1} \iint_{u_1 u_2} du_1 du_2 \partial\Xi_{u_1 u_2}(\lambda)/\partial\lambda|_{\lambda=0}$ being the geometric flux induced by the optomechanical Berry-phase-like effect of $\mathcal{G}_{\mathrm{geom}}$. Furthere, consider a specific modulation setup that the phase changes temporally, i.e., $\theta(t) = \theta_0 + 2\pi t/T_p$, the real part $M_s^R(t) = (1/2)\sinh(2r)\cos\theta(t)$ and the imaginary part $M_s^I(t) = (1/2)\sinh(2r)\sin\theta(t)$ change periodically. In this case, using
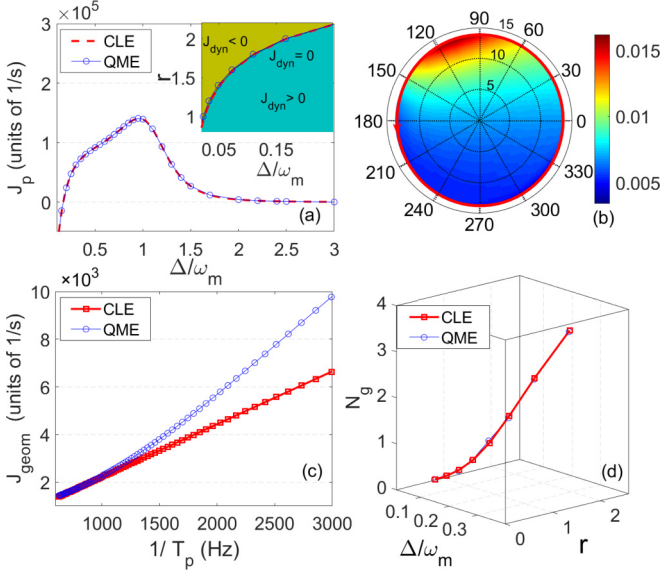
FIG. 3. (a) J_{dyn} as a function of Δ/ω_m with $r = 2.0$ and $T = 0.02$. (Inset) Contour of the transition point of J_{dyn} vs r and Δ/ω_m. (b) $\mathcal{F}(\mathcal{R}, \theta)$ as a function of θ and (c) J_{geom} as a function of $1/T_p$ at $J_{\mathrm{dyn}} \simeq 0$ with $r = 2.0$, $T = 0.02\,\mathrm{K}$, and $\Delta/\omega_m = 0.16688$, where the red ring is the modulation trajectory. (d) N_g as a function of r when $J_{\mathrm{dyn}} = 0$. The exact results of QME are well fitted by the analytical results in Eqs. (63) and (65) evaluated by the CGF approach. Other parameters are the same as those in Fig. 2(a).

the dynamical CGF $\mathcal{G}_{\mathrm{dyn}}$, the flux J_{dyn} reads

$$J_{\mathrm{dyn}} = -\gamma_m p_s^2 + \frac{1}{4\pi} \int_{-\infty}^{\infty} d\omega [\mathrm{Tr}(D_1 \Upsilon_n(\omega))], \quad (63)$$

which is independent of time due to the periodicity of $M_s^{(I, R)}(t)$. Here, D_1 is obtained by making $M_s^{R, I} = 0$ in matrix D_0. In particular, using $(u_1(t), u_2(t)) = (M_s^I(t), M_s^R(t))$ and Eq. (62), we have

$$\frac{\partial \Xi_{M_s^R M_s^I}}{\partial \lambda} \bigg|_{\lambda=0} = \frac{1}{2}\mathrm{Tr}\left[\left(\frac{\partial H_{20}^T}{\partial M_s^R}\frac{\partial H_{10}}{\partial M_s^I} - \frac{\partial H_{20}^T}{\partial M_s^I}\frac{\partial H_{10}}{\partial M_s^R}\right)H_{10}^{-1}\right]$$

$$\times \frac{1}{2}\mathrm{Tr}\left[\left(\frac{\partial H_{10}}{\partial M_s^R}H_{10}^{-1}\frac{\partial H_{10}}{\partial}M_s^I \right.\right.$$

$$\left.\left. - \frac{\partial H_{10}}{\partial M_s^I}H_{10}^{-1}\frac{\partial H_{10}}{\partial M_s^R}\right)H_{10}^{-1}H_{20}^T\right], \quad (64)$$

where $H_{20} = \lim_{\epsilon\to 0}\int_{-\infty}^{\infty}-\frac{d\omega}{2\pi}e^{-i\omega\epsilon}a_1'^{\dagger}D_0\phi$ with $a_1' = a_1/\lambda$ and $H_{10} = \int_{-\infty}^{\infty}\frac{d\omega}{2\pi}\rho^T D_0\phi$. The integral function [Eq. (64)] can also be seen as a function of the squeezing strength r and phase θ, i.e., $\mathcal{F}(\mathcal{R}, \theta) \equiv \partial\Xi_{M_s^I M_s^R}(\lambda)/\partial\lambda|_{\lambda=0}$ with $\mathcal{R} = (1/2)\sinh(2r)$. Then, the geometric flux induced by the optomechanical Berry-phase-like effect can be written as

$$J_{\mathrm{geom}} = T_p^{-1} \int_0^{\mathcal{R}} \int_{\theta_0}^{\theta_0+2\pi} \mathcal{F}(\mathcal{R}, \theta)\mathcal{R}d\mathcal{R}d\theta. \quad (65)$$

Figure 3(a) shows the dynamical flux J_{dyn} and its transition point from positive to negative values as a function of Δ/ω_m and r. We can see that the analytical result [Eq. (63)] from the CGF approach are well fitted by one numerical simulation in terms of the QME approach (see Appendix). We also focus
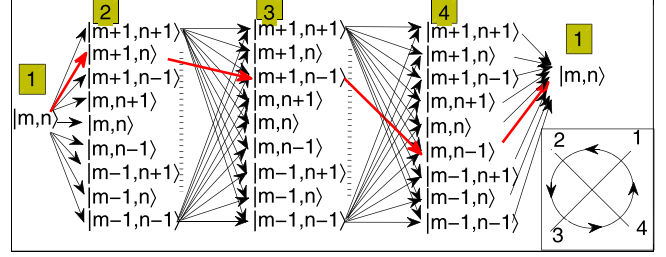

FIG. 4. A schematic representation of the level transitions and the squeezing modulation with the time-dependent phase $\theta(t)$ (inset).

on the generation of J_{geom} as $J_{\mathrm{dyn}} \simeq 0$ due to the adiabatic manipulation of θ, which leads to nonzero values of $\mathcal{F}(\mathcal{R}, \theta)$, portrayed in Fig. 3(b). Figure 3(c) shows that in the adiabatic limit the analytical result, i.e., $J_{\mathrm{geom}} = 2.2163 \times 1/T_p$ with $r = 2.0$ in Eq. (65), is consistent with the numerical computation. In the simulation the geometric thermo-phonon per cycle N_g already reaches the adiabatic limit when $T_p \gg \tau_\gamma = 159.15\,\mu\mathrm{s}$ with $\gamma_m = 2\pi \times 1000\,\mathrm{Hz}$, i.e., $T_p > 1000\,\mu\mathrm{s}$. Figure 3(d) shows that N_g increases with the increase of r, which plays the role of modulation amplitude of the noise. In particular, we see from Fig. 3(d) that N_g can be less than 1, which means that the geometric phonon response across the macroscopic mechanical motion near the quantum regime can be achieved.

From the thermodynamic point of view, this geometric pumping in the optomechanical system induced by the Berry-phase-like effect results from the dynamical engineering of the effective squeezed heat bath for the mechanical oscillator. The underlying physical mechanism can also be understood from the transition in optical and mechanical states near the quantum regime. We first assume that the system is in an equilibrium steady state, i.e., $|m, n\rangle$ in Fig. 1(b), without net energy exchange from the thermal bath to the system. In Fig. 4, according to the coupling in the system we list all transition paths in a cycle, where we simply divide the dynamical process into four stages marked with nodes 1, 2, 3 and 4, with 1 denoting the beginning state $|m, n\rangle$; and 2, 3 and 4 being nine adjacent intermediate states. The probability of a complete cyclic transition path, i.e., the path marked with red arrows in Fig. 4, can be calculated as $\rho_{m,n\to m+1,n}^{12}\rho_{m+1,n\to m+1,n-1}^{23}\rho_{m+1,n-1\to m,n-1}^{34}\rho_{m,n-1\to m,n}^{41}$ with $\rho_{m,n\to m+1,n}^{12}$ denoting the transition probability from $|m, n\rangle$ to $|m + 1, n\rangle$ during $1 \to 2$ and so on. The path will lead to that $\rho_{m,n-1\to m,n}^{41} - \rho_{m+1,n\to m+1,n-1}^{23}$ phonons are absorbed from the thermal bath. In addition to the paths that absorb phonons, there are also paths that emit phonons or do not exchange phonons with thermal bath. The equilibrium state ensures that the total absorbed phonons equals that of emission in the long time limit so that on average a net flux vanish.

Now we consider a cyclic regulation of the system. As shown in Fig. 3(b), the time-dependent reference phase $\theta(t)$ results in periodic changes of the vacuum noise environment in photon-number squeezed state and phase squeezed state, denoted by the nodes 1, 3 and 2, 4 in inset of Fig. 4, respectively. Correspondingly, the transition probabilities of sub-stages illustrated in Fig. 4 are controlled optically by the vacuum noise fluctuation. For example, for the red arrows'

in Fig. 4, the probability $\rho^{12}_{m,n\to m+1,n}$ may increase compared to the case without the modulation because it is more likely to gain photons from the optical bath enhanced by the photon-number fluctuation during $1\to 2$. As a result, the probability of the phonon loss to the thermal bath $\rho^{23}_{m+1,n\to m+1,n-1}$ in the following stage will be raised due to a larger dwelling probability in $|m+1,n\rangle$. In contrast, the probability $\rho^{34}_{m+1,n-1\to m,n-1}$ in the third stage may decrease because the loss of photons to the enhanced optical bath is suppressed and hence the probability of the phonon gain $\rho^{41}_{m,n-1\to m,n}$ in the forth stage will fall. Then, in the presence of the noise modulation, the number of phonon exchange $\rho^{41}_{m,n-1\to m,n}-\rho^{23}_{m+1,n\to m+1,n-1}$ reduces so that fewer phonons are absorbed from the thermal bath. Similarly, the transition probabilities of all the other possible cyclic paths can be changed by the modulation of the photon number and therefore the number of phonon exchange between the system and the thermal bath may rise or lower so that the absorption of phonons no longer offset the emission. That is, the optomechanical Berry-phase-like effect results from the fact that the transitions associated with the absorption of phonons from the thermal bath cannot compensate for the transitions associated with the emission of phonons to the thermal bath so that on average, the net energy transfer between the system and the thermal bath appears. The results suggest that the geometric flux induced by the Berry-phase-like effect provides a useful perspective for demonstrating the characteristics of a macroscopic mechanical motion near the quantum regime.

Noted that in order to observe experimentally the energy transfers, a system working in the good-cavity regime with $\kappa\ll\omega_m$ is advantageous. This is because the relative large coherence time ensures that the energy levels of the quantum system are sideband resolvable so that the transitions between different quantum states are distinguishable and the net energy transfer can be generated easily. In the opposite direction, i.e., $\kappa\gg\omega_m$, the transitions between different quantum states will be indistinguishable and the net energy transfer is still missing. Further, the geometric thermo-phonon pumping in the quantum regime demands that the modulation strength of the parameter should be relatively small so that only the quantum states adjacent to the initial state $|m,n\rangle$ are excited. Moreover, when the coupled oscillator system described by the analogous dynamical equation, i.e., Eq. (6), works in a classical regime with a large thermal noise strength (i.e., very high temperature of the mechanical oscillator), the geometric pumping number N_g will be much larger than 1 due to the large thermal fluctuations. We also stress that the dynamical control of the system can also be realized by using other periodically driven pairs $(u_1(t),u_2(t))$ in Eq. (62), i.e., two-color pump or amplitude modulated pump laser and the modulation of other optical parameters. Henceforth, an experimental verification of the characteristics of the energy rectification in a quantum optomechanical system is expected to be feasible using well-designed all-optical schemes [46].

VI. CONCLUSIONS

In summary, we have derived the general expression of the optomechanical Berry curvature and phase and studied in detail its impact on the thermo-phonon transport in a two-mode quantum optomechanical system. We find that the optome-

chanical Berry-phase-like-induced energy transfer is realized through the geometric phonon exchange, which is verified by the numerical results of the QME computation. The methods and results can be straightforwardly extended to the study of energy transport of multimode coupled oscillator systems and thereby open a new perspective for the energy rectifications in optomechanical systems with large mass oscillator and entropy production or the understanding of fluctuation theorem [46,72,82,83] of an out-of-equilibrium CV quantum system [26]. Our work can also be utilized to study the nonreciprocal energy transfer of other micro/nanoscale non-Hermitian systems with gain environment [84,85] as well as the quantum coherence control of flow in a hybrid optomechanical device with atomic ensembles or spins and other nonlinear optical media [86–89].

APPENDIX: QUANTUM MASTER EQUATION (QME) APPROACH

In this section, we use the quantum master equation to evaluate the thermo-phonon flux in the system. With the linearized Hamiltonian, the quantum master equation describing the evolution of the density matrix of the coupled oscillator system reads [68]

$$
\begin{aligned}
\dot{\rho} = {} & i[\rho, \Delta\delta\hat{a}^\dagger\delta\hat{a}+\omega_m\delta\hat{b}^\dagger\delta\hat{b}-G_1(\delta\hat{a}^\dagger+\delta\hat{a})(\delta\hat{b}^\dagger+\delta\hat{b})] \\
& + \gamma_m n_t(2\delta\hat{b}^\dagger\rho\delta\hat{b}-\delta\hat{b}\delta\hat{b}^\dagger\rho-\rho\delta\hat{b}\delta\hat{b}^\dagger) \\
& + \gamma_m(n_t+1)(2\delta\hat{b}\rho\delta\hat{b}^\dagger-\delta\hat{b}^\dagger\delta\hat{b}\rho-\rho\delta\hat{b}^\dagger\delta\hat{b}) \\
& + \kappa N_s(2\delta\hat{a}^\dagger\rho\delta\hat{a}-\delta\hat{a}\delta\hat{a}^\dagger\rho-\rho\delta\hat{a}\delta\hat{a}^\dagger) \\
& + \kappa(N_s+1)(2\delta\hat{a}\rho\delta\hat{a}^\dagger-\delta\hat{a}^\dagger\delta\hat{a}\rho-\rho\delta\hat{a}^\dagger\delta\hat{a}) \\
& + \kappa M_s(2\delta\hat{a}\rho\delta\hat{a}-\delta\hat{a}\delta\hat{a}\rho-\rho\delta\hat{a}\delta\hat{a}) \\
& + \kappa M_s^*(2\delta\hat{a}^\dagger\rho\delta\hat{a}^\dagger-\delta\hat{a}^\dagger\delta\hat{a}^\dagger\rho-\rho\delta\hat{a}^\dagger\delta\hat{a}^\dagger).
\end{aligned}
\tag{A1}
$$

It is noted that the present optomechanical Hamiltonian is linear, so it does not mix moments with different orders. As a result, in order to calculate thermo-phonon flux, it is not necessary to calculate all the matrix elements of the density operator ρ, but only to determine the time evolution of all the independent second-order moments, such as $\langle\delta a^\dagger\delta a\rangle$, $\langle\delta\hat{b}^\dagger\delta\hat{b}\rangle$, $\langle\delta\hat{a}^\dagger\delta\hat{b}\rangle$, $\langle\delta\hat{a}\delta\hat{b}\rangle$, $\langle\delta\hat{a}^2\rangle$, $\langle\delta\hat{b}^2\rangle$ and their Hermitian conjugates [90]. The differential equations are given by

$$
\frac{d}{dt}\langle\delta\hat{a}^\dagger\delta\hat{a}\rangle = iG_1(\langle\delta\hat{a}^\dagger\delta\hat{b}\rangle-\langle\delta\hat{a}^\dagger\delta\hat{b}\rangle^*+\langle\delta\hat{a}\delta\hat{b}\rangle^*-\langle\delta\hat{a}\delta\hat{b}\rangle)
$$
$$
-2\kappa\langle\delta\hat{a}^\dagger\delta\hat{a}\rangle+2\kappa N_s,
\tag{A2}
$$

$$
\frac{d}{dt}\langle\delta\hat{b}^\dagger\delta\hat{b}\rangle = iG_1(-\langle\delta\hat{a}^\dagger\delta\hat{b}\rangle+\langle\delta\hat{a}^\dagger\delta\hat{b}\rangle^*+\langle\delta\hat{a}\delta\hat{b}\rangle^*-\langle\delta\hat{a}\delta\hat{b}\rangle)
$$
$$
-2\gamma_m\langle\delta\hat{b}^\dagger\delta\hat{b}\rangle+2\gamma_m n_t,
\tag{A3}
$$

$$\frac{d}{dt}\langle\delta\hat{a}^{\dagger}\delta\hat{b}\rangle = iG_1(\langle\delta\hat{a}^{\dagger}\delta\hat{a}\rangle - \langle\delta\hat{b}^{\dagger}\delta\hat{b}\rangle^* + \langle\delta\hat{a}^2\rangle^* - \langle\delta\hat{b}^2\rangle)$$
$$+[i(\Delta - \omega_m) - (\kappa + \gamma_m)]\langle\delta\hat{a}^{\dagger}\delta\hat{b}\rangle, \quad \text{(A4)}$$

$$\frac{d}{dt}\langle\delta\hat{a}\delta\hat{b}\rangle = iG_1(\langle\delta\hat{a}^{\dagger}\delta\hat{a}\rangle + \langle\delta\hat{b}^{\dagger}\delta\hat{b}\rangle^* + \langle\delta\hat{a}^2\rangle^* + \langle\delta\hat{b}^2\rangle + 1)$$
$$-[i(\Delta + \omega_m) + (\kappa + \gamma_m)]\langle\delta\hat{a}\delta\hat{b}\rangle, \quad \text{(A5)}$$

$$\frac{d}{dt}\langle\delta\hat{a}^2\rangle = 2iG_1(\langle\delta\hat{a}\delta\hat{b}\rangle + \langle\delta\hat{a}^{\dagger}\delta\hat{b}\rangle)$$
$$-2(i\Delta + \kappa)\langle\delta\hat{a}^2\rangle - 2\kappa M_s^*, \quad \text{(A6)}$$

$$\frac{d}{dt}\langle\delta\hat{b}^2\rangle = 2iG_1(\langle\delta\hat{a}\delta\hat{b}\rangle + \langle\delta\hat{a}^{\dagger}\delta\hat{b}\rangle) - 2(i\omega_m + \gamma_m)\langle\delta\hat{b}^2\rangle. \quad \text{(A7)}$$

In the above calculation, the cutoff of the density matrix is not necessary and therefore the solutions of the linear system of equations are exact. Correspondingly, we can evaluate the thermo-phonon flux using above exact solutions for the second-order moments. For the present quantum oscillator model, the thermo-phonon flux operator $\hat{J}_{p1}$ in terms of the expression of $N_{p0}(\tau)$ can be expressed as

$$\hat{J}_{p1}(t) = [\hat{\xi}_p(t) - \gamma_m\delta\hat{p}(t)]\delta\hat{p}(t). \quad \text{(A8)}$$

Moreover, using Eq. (2), the above thermo-phonon flux operator can be written as

$$\hat{J}_{p1}(t) = \frac{1}{2}[(\omega_m\delta\hat{q} - G\delta\hat{X} + \delta\dot{\hat{p}})\delta\hat{p} + \delta\hat{p}(\omega_m\delta\hat{q} - G\delta\hat{X} + \delta\dot{\hat{p}})]$$
$$\text{(A9)}$$

by defining the dimensionless quadrature operators of the cavity mode

$$\delta\hat{X} = \frac{\delta\hat{a} + \delta\hat{a}^{\dagger}}{\sqrt{2}}, \quad \text{(A10)}$$

$$\delta\hat{Y} = \frac{\delta\hat{a} - \delta\hat{a}^{\dagger}}{\sqrt{2}i}, \quad \text{(A11)}$$

and the position and momentum fluctuation operators of the mechanical oscillator

$$\delta\hat{q} = \frac{(\delta\hat{b} + \delta\hat{b}^{\dagger})}{\sqrt{2}}, \quad \text{(A12)}$$

$$\delta\hat{p} = \frac{(\delta\hat{b} - \delta\hat{b}^{\dagger})}{\sqrt{2}i}. \quad \text{(A13)}$$

Then, using the quantum master equation [Eq. (A1)], the quantum average of the thermo-phonon flux can be expressed

as

$$J_{p1}(t) = \frac{1}{2}\langle\omega_m(\delta\hat{q}\delta\hat{p} + \delta\hat{p}\delta\hat{q}) - 2G\delta\hat{X}\delta\hat{p}\rangle. \quad \text{(A14)}$$

Further, using Eqs. (A10), (A12), and (A13), the average flux becomes

$$J_{p1}(t) = \frac{\omega_m}{2}\left(\frac{\langle\delta\hat{b}^2\rangle - \langle\delta\hat{b}^2\rangle^*}{i}\right) - G_1\left(\frac{\langle\delta\hat{a}\delta\hat{b}\rangle - \langle\delta\hat{a}\delta\hat{b}\rangle^*}{i}\right.$$
$$\left. + \frac{\langle\delta\hat{a}^{\dagger}\delta\hat{b}\rangle - \langle\delta\hat{a}^{\dagger}\delta\hat{b}\rangle^*}{i}\right),$$
$$\text{(A15)}$$

where we have used $G = 2G_1$. In the regimes of weak optomechanical coupling and red detuning, the system finally reaches a steady state and the derivatives in Eqs. (A2)–(A7) all become zero. Furthermore, all independent second-order moments, i.e., $\langle\delta\hat{a}^{\dagger}\delta\hat{a}\rangle$, $\langle\delta\hat{b}^{\dagger}\delta\hat{b}\rangle$, $\langle\delta\hat{a}^{\dagger}\delta\hat{b}\rangle$, $\langle\delta\hat{a}\delta\hat{b}\rangle$, $\langle\delta\hat{a}^2\rangle$, $\langle\delta\hat{b}^2\rangle$, and their Hermitian conjugates in Eqs. (A2)–(A7) can be solved analytically, so that the flux J_{p1} can be obtained analytically. However, the explicit expressions are quite cumbersome and will not be given here. The numerical results of the total thermal phonon flux (J_p) are shown in Fig. 2(e) of the main text in comparison with the analytical results. In addition, when a cyclic time-dependent modulation is imposed adiabatically on the system, the second moments in Eqs. (A2)–(A7) change slowly with time and therefore the thermo-phonon flux J_{p1} in Eq. (A15) is time-dependent and should be evaluated numerically. Finally, the total average thermo-phonon flux including the part related to p_s in a cycle of T_p after the system reaches steady state is

$$J_p = T_p^{-1}\int_0^{T_p}\left[-\gamma_m p_s^2(t) + J_{p1}(t)\right]dt. \quad \text{(A16)}$$

In numerical simulation, we consider the temporal change of the phase of squeezing, i.e., $\theta(t) = \theta_0 + 2\pi t/T_p$. Correspondingly, the real part $M_s^R(t) = (1/2)\sinh(2r)\cos\theta(t)$ and the imaginary part $M_s^I(t) = (1/2)\sinh(2r)\sin\theta(t)$ change periodically. In this case, the first moment p_s does not depend on time and the flux is simplified as

$$J_p = -\gamma_m p_s^2 + T_p^{-1}\int_0^{T_p}J_{p1}(t)dt. \quad \text{(A17)}$$

In the main text, we can compare the analytical results of the thermo-phonon flux from the CGF approach with the numerical simulation of the above QME.

[1] I. Wilson-Rae, N. Nooshi, W. Zwerger, and T. J. Kippenberg, Phys. Rev. Lett. **99**, 093901 (2007).

[2] F. Marquardt, J. P. Chen, A. A. Clerk, and S. M. Girvin, Phys. Rev. Lett. **99**, 093902 (2007).

[3] C. Genes, D. Vitali, P. Tombesi, S. Gigan, and M. Aspelmeyer, Phys. Rev. A **77**, 033804 (2008).

[4] Y.-C. Liu, Y.-F. Xiao, X. S. Luan, and C. W. Wong, Phys. Rev. Lett. **110**, 153606 (2013).

[5] J. Chan, T. P. M. Alegre, A. H. Safavi-Naeini, J. T. Hill, A. Krause, S. Gröblacher, M. Aspelmeyer, and O. Painter, Nature (London) **478**, 89 (2011).

[6] D. Vitali, S. Gigan, A. Ferreira, H. R. Böhm, P. Tombesi, A. Guerreiro, V. Vedral, A. Zeilinger, and M. Aspelmeyer, Phys. Rev. Lett. **98**, 030405 (2007).

[7] C. Genes, A. Mari, P. Tombesi, and D. Vitali, Phys. Rev. A **78**, 032316 (2008).

[8] W. J. Nie, Y. H. Lan, Y. Li, and S. Y. Zhu, Phys. Rev. A **86**, 063809 (2012).

[9] M. C. Kuzyk, S. J. van Enk, and H. Wang, Phys. Rev. A **88**, 062341 (2013).

[10] Y. D. Wang and A. A. Clerk, Phys. Rev. Lett. **110**, 253601 (2013).

[11] X. Yang, Y. Ling, X. Shao, and M. Xiao, Phys. Rev. A **95**, 052303 (2017).

[12] Q. Zheng, J. Xu, Y. Yao, and Y. Li, Phys. Rev. A **94**, 052314 (2016).

[13] X. Y. Li, W. J. Nie, A. X. Chen, and Y. H. Lan, Phys. Rev. A **96**, 063819 (2017).

[14] G. Y. Li, W. J. Nie, X. Y. Li, M. C. Li, A. X. Chen, and Y. H. Lan, Sci. China-Phys. Mech. Astron. **62**, 100311 (2019).

[15] J. Li, S. Y. Zhu, and G. S. Agarwal, Phys. Rev. Lett. **121**, 203601 (2018).

[16] H. Jing, S. K. Özdemir, X. Y. Lü, J. Zhang, L. Yang, and F. Nori, Phys. Rev. Lett. **113**, 053604 (2014).

[17] E. E. Wollman, C. U. Lei, A. J. Weinstein, J. Suh, A. Kronwald, F. Marquardt, A. A. Clerk, and K. C. Schwab, Science **349**, 952 (2015).

[18] X. W. Xu, Y. J. Zhao, and Y. X. Liu, Phys. Rev. A **88**, 022325 (2013).

[19] M. Abdi and M. J. Hartmann, New J. Phys. **17**, 013056 (2015).

[20] P. Rabl, Phys. Rev. Lett. **107**, 063601 (2011).

[21] A. Kronwald and F. Marquardt, Phys. Rev. Lett. **111**, 133601 (2013)

[22] M. Ludwig, A. H. Safavi-Naeini, O. Painter, and F. Marquardt, Phys. Rev. Lett. **109**, 063601 (2012).

[23] X. Y. Lü, W. M. Zhang, S. Ashhab, Y. Wu, and F. Nori, Sci. Rep. **3**, 2943 (2013).

[24] K. Børkje, A. Nunnenkamp, J. D. Teufel, and S. M. Girvin, Phys. Rev. Lett. **111**, 053603 (2013).

[25] G. L. Wang, Y.-C. Lai, and C. Grebogi, Sci. Rep. **6**, 35381 (2016).

[26] M. Aspelmeyer, T. J. Kippenberg, and F. Marquardt, Rev. Mod. Phys. **86**, 1391 (2014).

[27] E. Gavartin, P. Verlot, and T. J. Kippenberg, Nat. Nanotechnol. **7**, 509 (2012).

[28] J. Liu and K.-D. Zhu, Phys. Rev. D **95**, 044014 (2017).

[29] R. A. Norte, M. Forsch, A. Wallucks, I. Marinković, and S. Gröblacher, Phys. Rev. Lett. **121**, 030405 (2018).

[30] J. T. Hill, A. H. Safavi-Naeini, J. Chan, and O. Painter, Nat. Commun. **3**, 1196 (2012).

[31] L. Tian, Ann. Phys. (Berlin) **527**, 1 (2015).

[32] S. Barzanjeh, S. Guha, C. Weedbrook, D. Vitali, J. H. Shapiro, and S. Pirandola, Phys. Rev. Lett. **114**, 080503 (2015).

[33] H. Xu, D. Mason, L. Jiang, and J. G. E. Harris, Nature (London) **537**, 80 (2016).

[34] X. Z. Zhang, L. Tian, and Y. Li, Phys. Rev. A **97**, 043818 (2018).

[35] K. Zhang, F. Bariani, and P. Meystre, Phys. Rev. Lett. **112**, 150602 (2014).

[36] K. Zhang, F. Bariani, and P. Meystre, Phys. Rev. A **90**, 023819 (2014).

[37] A. U. C. Hardal, N. Aslan, C. M. Wilson, and O. E. Müstecaplıoğlu, Phys. Rev. E **96**, 062120 (2017).

[38] D. G. Klimovsky and G. Kurizki, Sci. Rep. **5**, 7809 (2015).

[39] A. Mari, A. Farace, and V. Giovannetti, J. Phys. B **48**, 175501 (2015).

[40] M. Bathaee and A. R. Bahrampour, Phys. Rev. E **94**, 022141 (2016).

[41] K. Zhang and W. Zhang, Phys. Rev. A **95**, 053870 (2017).

[42] Y. Dong, F. Bariani, and P. Meystre, Phys. Rev. Lett. **115**, 223602 (2015).

[43] A. Xuereb, A. Imparato, and A. Dantan, New J. Phys. **17**, 055013 (2015).

[44] S. Barzanjeh, M. Aquilina, and A. Xuereb, Phys. Rev. Lett. **120**, 060601 (2018).

[45] A. Seif, W. DeGottardi, K. Esfarjani, and M. Hafezi, Nat. Commun. **9**, 1207 (2018).

[46] M. Brunelli, L. Fusco, R. Landig, W. Wieczorek, J. Hoelscher-Obermaier, G. Landi, F. L. Semião, A. Ferraro, N. Kiesel, T. Donner, G. De Chiara, and M. Paternostro, Phys. Rev. Lett. **121**, 160604 (2018).

[47] M. T. Naseem, A. Xuereb, and Ö. E. Müstecaplıoğlu, Phys. Rev. A **98**, 052123 (2018).

[48] D. Segal, Phys. Rev. Lett. **101**, 260601 (2008).

[49] Y. Dubi and M. Di Ventra, Rev. Mod. Phys. **83**, 131 (2011).

[50] A. Dhar and D. Roy, J. Stat. Phys. **125**, 801 (2006).

[51] A. Dhar, O. Narayan, A. Kundu, and K. Saito, Phys. Rev. E **83**, 011101 (2011).

[52] N. B. Li, J. Ren, L. Wang, G. Zhang, P. Hänggi, and B. Li, Rev. Mod. Phys. **84**, 1045 (2012).

[53] C. Wang, X. M. Chen, K. W. Sun, and J. Ren, Phys. Rev. A **97**, 052112 (2018).

[54] M. Terraneo, M. Peyrard, and G. Casati, Phys. Rev. Lett. **88**, 094302 (2002).

[55] D. Segal, Phys. Rev. Lett. **100**, 105901 (2008).

[56] R. Scheibner, M. König, D. Reuter, A. D. Wieck, C. Gould, H. Buhmann, and L. W. Molenkamp, New J. Phys. **10**, 083016 (2008).

[57] S. Basu and M. Francoeur, Appl. Phys. Lett. **98**, 113106 (2011).

[58] B. Li, L. Wang, and G. Casati, Phys. Rev. Lett. **93**, 184301 (2004).

[59] J. Ordonez-Miranda, Y. Ezzahri, and K. Joulain, Phys. Rev. E **95**, 022128 (2017).

[60] K. Joulain, J. Drevillon, Y. Ezzahri, and J. Ordonez-Miranda, Phys. Rev. Lett. **116**, 200601 (2016).

[61] L. Wang and B. Li, Phys. Rev. Lett. **99**, 177208 (2007).

[62] J. Ren, P. Hänggi, and B. Li, Phys. Rev. Lett. **104**, 170601 (2010).

[63] T. Yuge, T. Sagawa, A. Sugita, and H. Hayakawa, Phys. Rev. B **86**, 235308 (2012).

[64] T. Chen, X. B. Wang, and J. Ren, Phys. Rev. B **87**, 144303 (2013).

[65] J. Ren, S. Liu, and B. Li, Phys. Rev. Lett. **108**, 210603 (2012).

[66] S. Liu, B. K. Agarwalla, J. S. Wang, and B. W. Li, Phys. Rev. E **87**, 022122 (2013).

[67] C. Wang, J. Ren, and J. S. Cao, Phys. Rev. A **95**, 023610 (2017).

[68] M. O. Scully and M. S. Zubairy, *Quantum optics* (Cambridge University Press, Cambridge, 2011).

[69] D. Yu, L. C. Kwek, L. Amico, and R. Dumke, Phys. Rev. A **95**, 053811 (2017).

[70] A. Kundu, S. Sabhapandit, and A. Dhar, J. Stat. Mech. (2011) P03007.

[71] S. Sabhapandit, Phys. Rev. E **85**, 021108 (2012).

[72] D. Gupta and S. Sabhapandit, J. Stat. Mech. (2018) 063203.

[73] K. Jähne, C. Genes, K. Hammerer, M. Wallquist, E. S. Polzik, and P. Zoller, Phys. Rev. A **79**, 063819 (2009).

[74] A. Motazedifard, F. Bemani, M. H. Naderi, R. Roknizadeh, and D. Vitali, New J. Phys. **18**, 073040 (2016).

[75] A. Dalafi, M. H. Naderi, and A. Motazedifard, Phys. Rev. A **97**, 043619 (2018).

[76] N. A. Sinitsyn, J. Phys. A **42**, 193001 (2009).

[77] M. V. Berry, Proc. R. Soc. Lond. A **392**, 45 (1984).

[78] J. G. Garrison and E. M. Wright, Phys. Lett. A **128**, 177 (1988).

[79] L. Latmiral and F. Armata, Sci. Rep. **10**, 2264 (2020).

[80] W. J. Nie and Y. H. Lan, Phys. Rev. E **86**, 011110 (2012).

[81] N. A. Sinitsyn and I. Nemenman, Phys. Rev. Lett. **99**, 220408 (2007).

[82] K. Saito and A. Dhar, Phys. Rev. Lett. **99**, 180601 (2007).

[83] A. Bérut, A. Imparato, A. Petrosyan, and S. Ciliberto, Phys. Rev. Lett. **116**, 068301 (2016).

[84] R. El-Ganainy, K. G. Makris, M. Khajavikhan, Z. H. Musslimani, S. Rotter, and D. N. Christodoulides, Nat. Phys. **14**, 11 (2018)

[85] Z. P. Gong, Y. Ashida, K. Kawabata, K. Takasan, S. Higashikawa, and M. Ueda, Phys. Rev. X **8**, 031079 (2018).

[86] S. Camerer, M. Korppi, A. Jöckel, D. Hunger, T. W. Hänsch, and P. Treutlein, Phys. Rev. Lett. **107**, 223001 (2011).

[87] A. V. Parafilo, S. I. Kulinich, L. Y. Gorelik, M. N. Kiselev, R. I. Shekhter, and M. Jonson, Phys. Rev. Lett. **117**, 057202 (2016).

[88] D. A. Golter, T. Oo, M. Amezcua, K. A. Stewart, and H. Wang, Phys. Rev. Lett. **116**, 143602 (2016).

[89] P. Michler, A. Kiraz, C. Becher, W. V. Schoenfeld, P. M. Petroff, L. Zhang, E. Hu, and A. Imamoğlu, Science **290**, 2282 (2000).

[90] I. Wilson-Rae, N. Nooshi, J. Dobrindt, T. J. Kippenberg, and W. Zwerger, New J. Phys. **10**, 095007 (2008).